PNAS RESEARCH ARTICLE | MEDICAL SCIENCES

NOVA1 acts as an oncogenic RNA-binding protein to regulate cholesterol homeostasis in human glioblastoma cells

Yuhki Saito[a,b,1], Yanhong Yang[c,d], Misa Saito[a,b], Christopher Y. Park[a,b,2], Kosuke Funato[c,d,3], Viviane Tabar[c,d], and Robert B. Darnell[a,b,1]

Contributed by Robert B. Darnell; received September 1, 2023; accepted January 13, 2024; reviewed by Benjamin J. Blencowe and Adrian R. Krainer

NOVA1 is a neuronal RNA-binding protein identified as the target antigen of a rare autoimmune disorder associated with cancer and neurological symptoms, termed paraneoplastic opsoclonus-myoclonus ataxia. Despite the strong association between NOVA1 and cancer, it has been unclear how NOVA1 function might contribute to cancer biology. In this study, we find that NOVA1 acts as an oncogenic factor in a GBM (glioblastoma multiforme) cell line established from a patient. Interestingly, NOVA1 and Argonaute (AGO) CLIP identified common 3′ untranslated region (UTR) targets, which were down-regulated in NOVA1 knockdown GBM cells, indicating a transcriptome-wide intersection of NOVA1 and AGO–microRNA (miRNA) targets regulation. NOVA1 binding to 3′UTR targets stabilized transcripts including those encoding cholesterol homeostasis related proteins. Selective inhibition of NOVA1–RNA interactions with antisense oligonucleotides disrupted GBM cancer cell fitness. The precision of our GBM CLIP studies point to both mechanism and precise RNA sequence sites to selectively inhibit oncogenic NOVA1–RNA interactions. Taken together, we find that NOVA1 is commonly overexpressed in GBM, where it can antagonize AGO2–miRNA actions and consequently up-regulates cholesterol synthesis, promoting cell viability.

Nova1 | RNA-binding protein | glioblastoma | CLIP | cholesterol

Significance

Glioblastoma multiforme (GBM) is one of humankind's deadliest cancers with an average life expectancy of just over 1 y. This grim prognosis comes despite decades of research, which has established the value of intervention (surgery, radiation, and chemotherapy) over natural history (where diagnosis to death was measured in months) but has yet to take advantage of modern molecular knowledge and technologies. NOVA1, a neuronal RNA-binding protein (RBP) was found here to be critical for GBM cell fitness, oncogenic NOVA1-RNA interactions, and regulation of key target transcripts. These findings contribute to understanding the molecular basis of GBM and to the discovery of new drug targets.

NOVA1 was originally identified as an autoantigen of paraneoplastic neurologic diseases (PNDs), a rare group of diseases at the intersection of neurobiology, immunology, and oncology (1–3). Patients with PNDs harbor systemic tumors (e.g., breast, lung, bladder cancer, and neuroblastoma) and develop immune responses against onconeural antigens that are expressed both by their tumors and by normal neural cells (3, 4).

The prevailing model for the pathogenesis of PNDs (3, 5) sets the stage for considering the role of these proteins in cancer cells. This model postulates that PNDs are initiated by de novo expression of genes that are normally transcribed behind the blood–brain barrier, primarily and in some cases exclusively in neurons. The genes encoding the NOVA1 and NOVA2 PND autoantigens were cloned using patients antisera, revealing that these proteins and their transcripts are expressed exclusively in central nervous system neurons (1, 6). Although there may be exceptions to this "rule" [expression of Nova1 in pancreatic cells in vitro; (7, 8)], they appear to relate to expression in small groups of cells, some of which are of neural crest lineage (pancreatic beta cells) and hence may have unappreciated features of immune privilege.

This model further postulates that the inciting event in PND is the aberrant expression of onconeural antigens in cancer cells [typically in adult tumors; (3)]. This triggers an appropriate, and in some (or perhaps many) cases, naturally occurring effective anti-tumor immune responses (9). A paradox then arises. If tumor cells ectopically express a gene that puts them at risk for being seen as nonself by the immune system (4, 10, 11), why do they do so? The most straightforward hypothesis has been that such expression is selected because the protein product of those genes confers some pro-tumor advantage.

Here, we explore the biology of the PND antigen NOVA1 in the context of cancer cells. The NOVA antigens are associated with ectopic expression in breast or ovarian tumors and the paraneoplastic opsoclonus myoclonus ataxia syndrome (3, 12). We assessed the expression of NOVA1 mRNA in The Cancer Genome Atlas (TCGA) tumors, finding high levels of expression in breast cancer (BRCA), and unexpectedly, in glioblastoma. This prompted us to further explore whether NOVA1 might act on specific transcripts in human GBM-derived cell lines and whether such actions could contribute to the biology of the tumor cells in vitro and in animal models. Our findings reveal that NOVA1 is highly up-regulated in GBM cancer stem cells and a GBM cell line derived from a patient. In these cells, NOVA1 is able to antagonize AGO–miR interactions in target transcript 3′UTRs and thereby regulate their expression. Notably, this includes RNAs encoding proteins

Author contributions: Y.S., V.T., and R.B.D. designed research; Y.S., Y.Y., and M.S. performed research; K.F. contributed new reagents/analytic tools; Y.S., C.Y.P., and R.B.D. analyzed data; and Y.S. and R.B.D. wrote the paper.

Reviewers: B.J.B., University of Toronto; and A.R.K., Cold Spring Harbor Laboratory.

Competing interest statement: R.B.D. is a consultant for Atreca, Inc. and OPNA IO, LLC, and is a founder of a nonprofit (Permantis Public Health) for which he has no financial stake.

[1]To whom correspondence may be addressed. Email: ysaito@rockefeller.edu or darnelr@rockefeller.edu.

[2]Present address: Flatiron Institute, Simons Foundation, New York, NY 10010.

[3]Present address: Department of Biochemistry and Molecular Biology, University of Georgia, Athens, GA 30602.

This article contains supporting information online at https://www.pnas.org/lookup/suppl/doi:10.1073/pnas.2314695121/-/DCSupplemental.

Published February 28, 2024.

involved in cholesterol synthesis, with consequences for GBM cell growth suggesting new avenues for therapeutic development.

Results

NOVA1 as an Oncogenic RNA-Binding Protein (RBP) in GBM. In the course of screening for potentially oncogenic RBPs, we unexpectedly found that NOVA1 has the highest level of overexpression (OE) in GBM cancer stem-like cells compared to differentiated glioma cells (*SI Appendix*, Fig. S1*A*: re-analysis of data in ref. 13). To investigate more generally what type of cancers express NOVA1, we explored TCGA RNAseq (RNAsequencing) data. A limited set of cancers overexpress NOVA1, notably BRCA, low-grade glioma, and glioblastoma multiforme (GBM) (Fig. 1*A*).

In mice, NOVA1 functions in the normal brain have been well studied (14–20). However, its roles in human cancer cells including GBM are unexplored. In order to investigate this, we conducted a viability assay on a GBM cell line, MSK-19, derived from a patient with GBM (Fig. 1*B*). The viability of GBM cells over-expressing NOVA1 and shRNAs targeting *NOVA1* were very significantly increased and decreased, respectively, when compared with control MSK-19 cells expressing nontargeting shRNA (Fig. 1*B* and *SI Appendix*, Fig. S1*B*). To test whether NOVA1 plays a role in tumorigenicity, MSK-19 cells were labeled with luciferase and transplanted intracranially into Immunodeficient mice (Fig. 1*C*). All animals in the control group reached endpoint clinical criteria by 80 d (Fig. 1*D*). In contrast, survival of animals transplanted with MSK-19 cells in which NOVA1 had been knocked down (KD) was significantly increased (Fig. 1*D*). Taken together, these results demonstrate a critical role played by NOVA1 in the fitness and tumorigenesis of GBM cells.

Identification of NOVA1 Target Transcripts in GBM and Selective Inhibition of NOVA1-Target Interactions. To explore NOVA1 targets in GBM cells, we took advantage of CLIP technology (21–23), which precisely identifies transcriptome-wide targets of RBPs by UV-induced crosslinking proteins to RNA followed by high-throughput sequencing (Fig. 2*A*). NOVA1 CLIP assays in MSK-19 yielded a single autoradiographic band at the expected size of NOVA1 (55 kDa) in high RNase A-treated and UV cross-linked cell extracts (Fig. 2*A*, second lane). This signal was absent in controls that were not UV-crosslinked (Fig. 2*A*, first lane). The expected extended range of signals was detected in UV cross-linked GBM cell extracts treated with low doses of RNase A (Fig. 2*A*, third and fourth lanes).

We performed four CLIP replicates to generate a total of 18,787,637 unique NOVA1 CLIP tags (*SI Appendix*, Fig. S2*A*). This analysis yielded 87,610 significant peaks with filters for $P < 0.05$, peak height (PH) ≥ 10, and biological complexity/replicates = 4. Motif analysis in cross-linking-induced mutation sites (24) identified enrichment of UCAU motifs in NOVA1-bound peaks, as previously reported (*SI Appendix*, Fig. S2*B*). In addition, 81.7% of NOVA1 CLIP peaks were located within the intron of transcripts, and 13.1% were within 3′UTR (Fig. 2*B*).

To investigate the effect of NOVA1 loss-of-function on target transcripts in MSK-19 cells, the extracted RNAs from a control and two *NOVA1*-KD (NOVA1-KD1 and -KD2) independent MSK-19 cell lines generated with different shRNAs were subjected to RNAseq analysis. This identified 428 and 164 genes which were commonly down- or up-regulated, respectively, in all biological replicates of both NOVA1-KD1 and -KD2 MSK-19 cells when compared with control MSK-19 cells (FDR < 0.05 and $\log_2$ fold

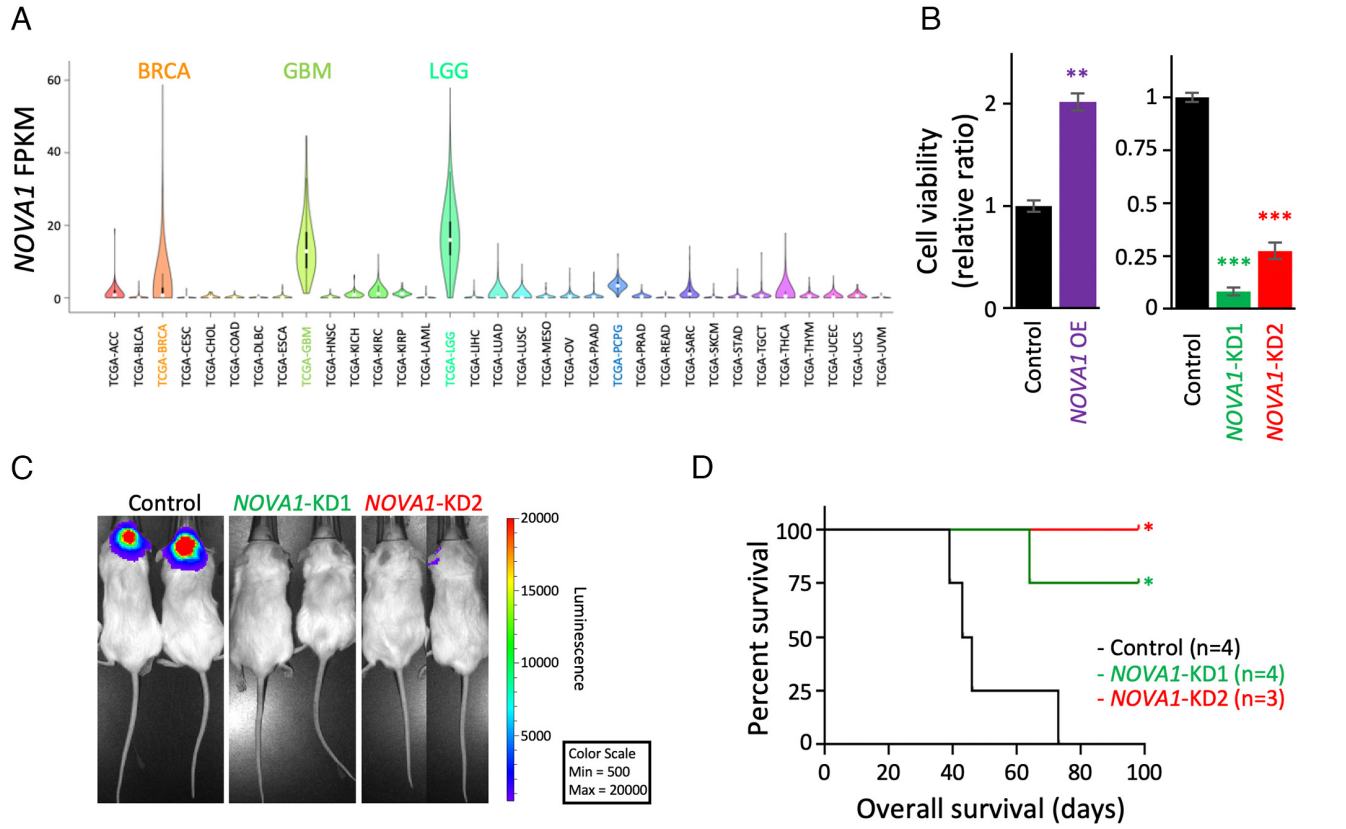

Fig. 1. Expression and functions of an RBP NOVA1 in tumors. (*A*) NOVA1 mRNA expression in a series of TCGA tumors. *Y*-axis indicates FPKM value of NOVA1. (*B*) Cell viability of GBM cells derived from a patient in the condition of NOVA1 OE (*Left*) and NOVA1 knockdown (KD, *Right*). n = 3 (*Left*) and n = 4 (*Right*) biologic replicates. $^{**}P < 0.01$, $^{***}P < 0.001$, *t* test). (*C* and *D*) In vivo growth of NOVA1-KD GBM cells visualized with bioluminescence imaging (*C*) and survival analysis (Kaplan–Meier curve) of mice (NOD-SCID) bearing the human GBM tumors (n ≥ 3, $^{*}P < 0.05$, Gehan–Breslow–Wilcoxon test).

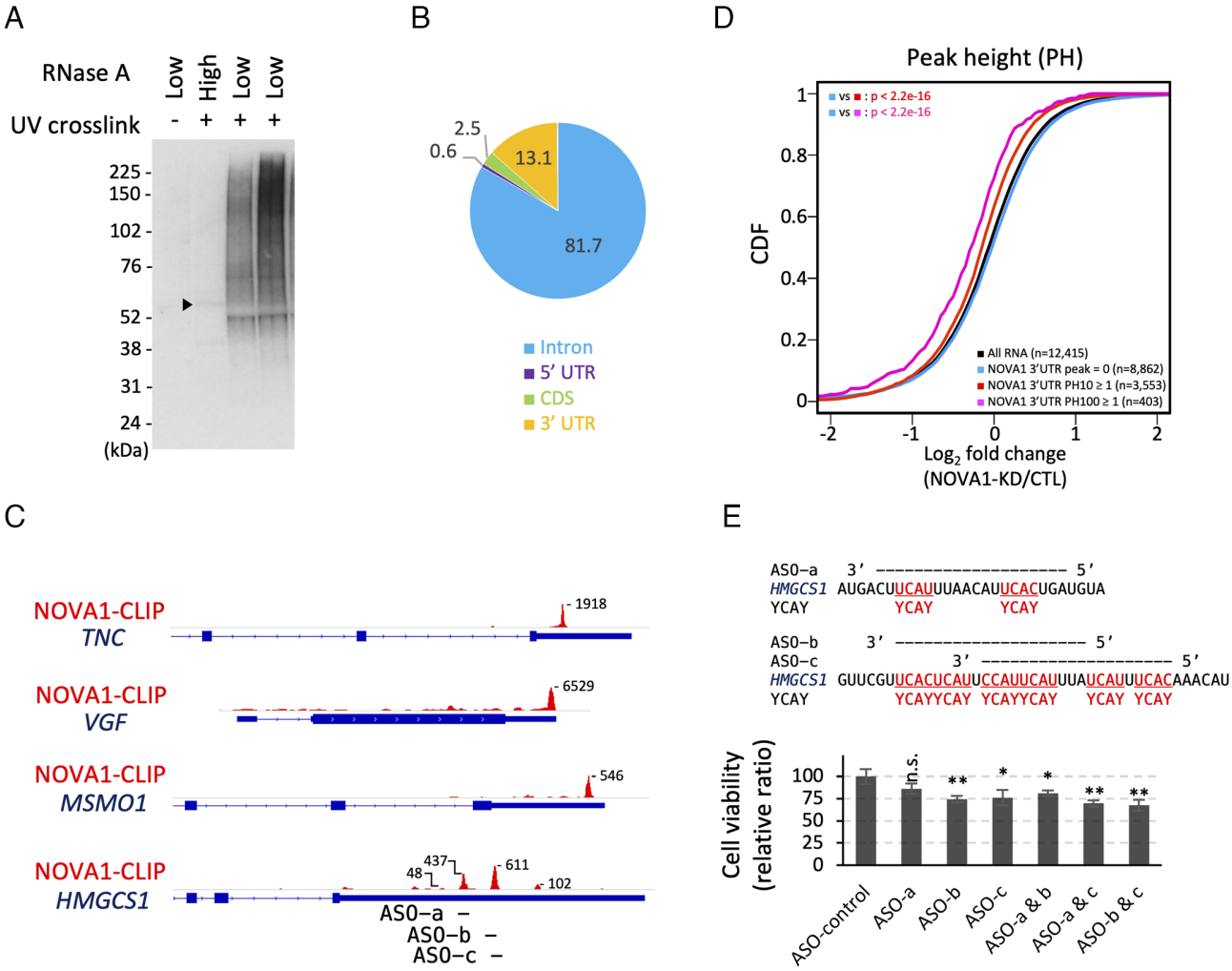

Fig. 2. Identification of NOVA1 targets with CLIP in human GBM cells derived from a patient and the inhibition of NOVA1-RNA interactions. (*A*) Autoradiograph images of NOVA1 CLIP samples labeled with T4 polynucleotide kinase and γ-32P adenosine triphosphate (ATP). (*B*) Distribution of NOVA1 CLIP peak locations across genic regions. (*C*) Genome browser view of examples for NOVA1 3′UTR targets. (*D*) Cumulative density function (CDF) plots of NOVA1-KD RNAseq. Curves represent collective changes among NOVA1 3′UTR targets binned by peak height (PH); n indicates number of targets. Mann–Whitney′ test. (*E*) GBM cell survival assay treated with ASOs that occupy NOVA1 binding sites. Then, 0.5 pmol ASOs were treated for 5 d by free uptake. n = 3, $*P < 0.05$, $**P < 0.01$, *t* test.

change (FC) > 0 or < 0; *P* values < 10^{-100} by hypergeometric tests). Alternative splicing analysis identified 147 alternative splicing events altered in *NOVA1*-KD MSK-19 cells. The number and degree of splicing changes in *NOVA1*-KD MSK-19 cells was slight and similar to changes in *Nova1*-KO mouse brain data (16, 25). Integration of both NOVA1 CLIP and *NOVA1*-KD RNAseq data identified 149 direct NOVA1 targets whose expression levels were down- (117 targets) or up- (32 targets) regulated in *NOVA1*-KD MSK-19 cells. NOVA1 directly bound to the 3′UTRs of transcripts of 65 of 117 down-regulated genes (e.g., TNC, VGF, MSMO1, HMGCS1 in Fig. 2*C*) and the 3′UTRs of transcripts of 4 of 32 up-regulated genes (*SI Appendix*, Fig. S2 *C* and *D*), consistent with prior observations of NOVA proteins acting on 3′UTRs in brain transcripts (25–27).

Cumulative distribution function plots of RNAseq $\log_2$ FC (*NOVA1*-KD/control) showed a significant global reduction in NOVA1 3′UTR targets; this correlates with NOVA1 CLIP PH (Fig. 2*D*) and peak number (*SI Appendix*, Fig. S2*E*). To investigate whether the targeted inhibition of NOVA1–RNA interaction has effects on GBM cell fitness, we designed three antisense oligonucleotides (ASOs a-c) of 20 nucleotide length with 2′-*O*-Methyl and phosphorothioate modifications for *HMGCS1*, which encodes a key enzyme in the cholesterol synthesis pathway (Fig. 2*E*). Cell viability was significantly reduced in cells treated with ASO-b, -c, or a combination of two ASOs (Fig. 2*E*). These results support our hypothesis that direct NOVA1 binding to transcript 3′UTRs could regulate the stability of targets as well as cell viability.

Intersection of NOVA1 and AGO–miRNA (microRNA) in Human GBM Cell. We reported that Nova1 antagonizes the actions of miRNAs (e.g. miR-124, miR-139) on 3′UTR of *Impact* in the mouse neurons (20). However, transcriptome-wide intersections of NOVA1 with miRNAs have not been systematically investigated. To explore this, we performed four AGO CLIP assays by utilizing post-NOVA1 CLIP cell lysates used in Fig. 2*A* and *SI Appendix*, Fig. S3*A*. A total of 6,523,201 unique AGO CLIP tags were obtained and 236,984 unique tags were mapped onto transcripts including mRNA and miRNA (*SI Appendix*, Fig. S3*B*). This analysis yielded 24,425 significant peaks ($P < 0.05$, PH ≥ 10, and biological complexity/replicates = 4). Then, 50.7% of AGO CLIP peaks were located within the 3′UTR of mRNA transcripts, and 31.9% and 15.0% were within intron and CDS, respectively (Fig. 3*A*), consistent with AGO CLIP maps found in mouse brain (28). Following that, 173 AGO CLIP peaks were mapped onto miRNA. The top five miRNA ranked by unique AGO CLIP

tag number were *MIR374A*, *MIR374B*, *MIR21*, *MIR26B*, and *MIR19A*.

A total of 2,786 genes had both AGO and NOVA1 CLIP peaks in their 3′UTR of transcripts (Fig. 3*B*). Fifty-nine of 65 down-regulated genes in NOVA1-KD GBM cells (*SI Appendix*, Fig. S2*C*, including the top ranked targets *TNC*, *VGF*, *HMGCS1*, *MSMO1*) were 3′UTR targets of both AGO and NOVA1 RBPs (Fig. 3*C*). As an example, *MSMO1*, encoding a protein also involved in cholesterol synthesis (29, 30), was down-regulated in NOVA1-KD GBM cells. MSMO1 transcripts harbor overlapping NOVA1 and AGO CLIP 3′UTR peaks (peak separation of less than 100 nt; Fig. 3*D*). Moreover, a *Mir19A-3p* seed predicted with TargetScan was located in the AGO CLIP peak on *MSMO1* 3′UTR and unique AGO CLIP tags were detected in *Mir19A* locus (Fig. 3*E*). Taken together, these results suggest that NOVA1 may antagonize the effect of AGO–*Mir19A* on *MSMO1* in normal cells or when overexpressed in GBM cells, leading to an upregulation of cholesterol synthesis.

Transcriptome-wide analysis revealed both NOVA1 and AGO-dependent down-regulation of target genes in NOVA1-KD GBM cells (Fig. 3*F*). The abundance of NOVA1 or AGO 3′UTR targets was moderately reduced in GBM cells in which NOVA1 had been knocked down (columns 2 to 7 in Fig. 3*F*). No significant change was detected in genes harboring only NOVA1 3′UTR

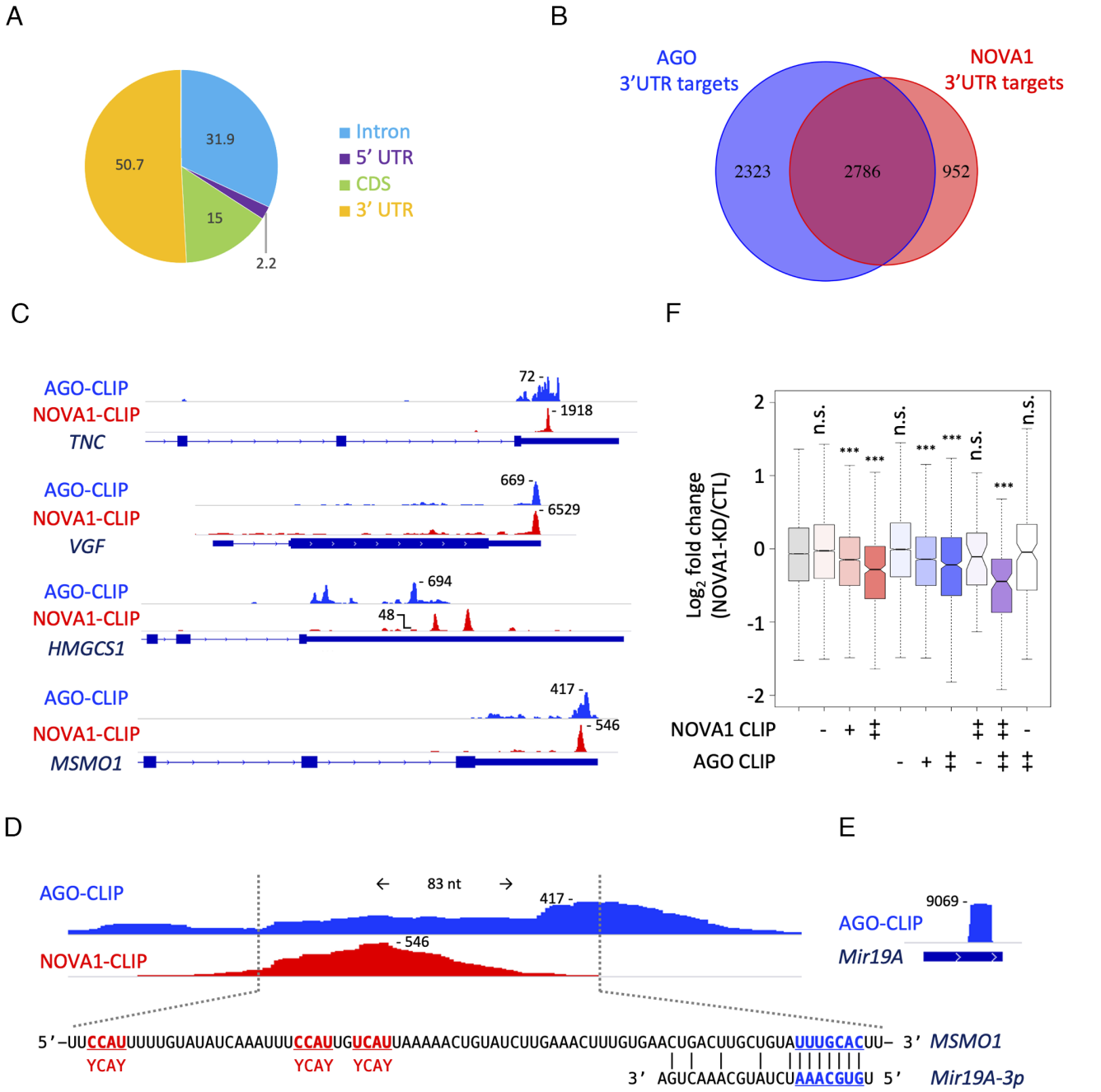

Fig. 3. Intersection of down-regulated NOVA1 3′UTR targets in NOVA1-KD GBM cells with AGO–miRNA targets. (*A*) Distribution of AGO CLIP peak locations across genic regions. Numbers indicate the percentage. (*B*) Venn diagram representing the number of AGO and NOVA1 3′UTR targets overlapping or differential between two RBPs. (*C*) Genome browser view of examples for both NOVA1 and AGO 3′UTR targets down-regulated in NOVA1-KD GBM. (*D*) Magnified genome browser view and sequences of MSMO1 and Mir19A-3p RNAs. NOVA1 binding motifs (YCAY) and miRNA seed sequence were highlighted with red and blue, respectively. (*E*) Genome browser view of AGO–CLIP on Mir19A. (*F*) RNAseq fold change delineated by NOVA1 and AGO 3′UTR targets and CLIP PH. + and ++ indicate CLIP PH ≥ 10 and ≥ 100, respectively.

targets (column 8 in Fig. 3*F*) or AGO 3′UTR targets (column 10 in Fig. 3*F*). Interestingly, genes of both NOVA1 and AGO 3′UTR targets (column 9 in Fig. 3*F*) were more severely affected in NOVA1-KD cells, supporting a model in which NOVA1 normally antagonizes the actions of the AGO–miRNA complex.

Dysregulation of Cholesterol Biosynthetic Process in NOVA1-KD GBM Cells. To explore the biological pathways regulated by NOVA1 in GBM cells, we analyzed the targets encoded by significantly down- and up-regulated genes in *NOVA1*-KD GBM cells by GO analysis. This revealed significant enrichment of both cholesterol biosynthetic and glycolysis process terms in the NOVA1-KD down-regulated genes (Fig. 4*A*). Several lines of evidence revealed that brain cancers including GBM are remarkably dependent on cholesterol for survival and vulnerable to agents that act to agonize the Live X receptor (LXR). LXR is a transcription factor that acts to promote cholesterol efflux through upregulation of sterol transporters such as ABCA1, and suppress influx through IDOL/MYLIP-mediated degradation of low-density lipoprotein receptor (31–34). qPCR analysis revealed significant changes in several transcripts known to be up-regulated upon LXR activation (e.g., E3 ligase *MYLIP/IDOL*, *ABCG1* cholesterol efflux transporter, *ABCA1* cholesterol efflux transporter) (Fig. 4*B*). These results in NOVA-KD GBM cells reveal a net action of NOVA1 to maintain cholesterol homeostasis in GBM cells.

To test whether disruption of cholesterol homeostasis is functionally impacted by NOVA1-KD, we assessed cell death in cells cultured with or without exogeneous cholesterol. Provision of exogenous cholesterol partially rescued cell death evident in *NOVA1*-KD cells (Fig. 4*C*). Taken together, these data suggest that NOVA1 is able to act in GBM cells to increase cholesterol homeostasis that is essential for GBM cell survival and that disruption of NOVA1 action can kill GBM cells.

Discussion

NOVA1 was originally identified as targets in paraneoplastic opsoclonus–myoclonus-ataxia but its roles in cancers were unclear. In the present work, we have found that an RBP, NOVA1, acts as an oncogenic factor and regulates cholesterol homeostasis in a low passaged GBM cell line established from a patient. Our previous work identified the downregulation of metabolic pathways such as cholesterol in the brain of inhibitory neuron-specific *Nova1*-cKO mice (20), indicating that NOVA1 regulates the cholesterol metabolic pathway in the mouse brain. Here, we extend these observations in the context of cancer.

Our unbiased screen for NOVA 1 targets in human GBM cells here again identifies a biologic role for NOVA1 in regulating transcripts encoding key factors in cholesterol synthesis. As was the case in mouse inhibitory neurons, NOVA1 action in human GBM cells appears to regulate this pathway through binding to 3′UTRs. While NOVA1 was originally identified through its action on alternative splicing in mouse brain (16, 26), we have also identified functional binding in mouse the 3′UTR (26), and specifically the action of NOVA1 in inhibitory diencephalic neurons grown in vitro (20). Here, CLIP analysis reveals that the bulk of NOVA1 CLIP binding in human GBM transcripts was to 3′UTR elements. Moreover, consistent with the detailed study of NOVA1 action on the *Impact* 3′UTR in mouse diencephalic neurons (20), our systematic search for NOVA1 binding in glioma cell 3′UTRs revealed that this

A

Term	p-Value	Genes
GO:0006695 - cholesterol biosynthetic process	3.42E-10	*FDPS, IDI1, ACLY, EBP, MVK, HMGCS1, INSIG1, MSMO1, DHCR24, DHCR7, HSD17B7, LSS*
GO:0061621 - canonical glycolysis	5.46E-08	*GPI, PFKFB4, PKM, PGK1, ENO1, GAPDH, HK2, PFKP, HK1*
GO:0006096 - glycolytic process	7.41E-06	*GPI, LDHA, OGDH, PGK1, ENO1, GAPDH, HK2, HK1*
GO:0006094 - gluconeogenesis	3.72E-04	*GPI, G6PC3, GOT1, PGK1, ENO1, SLC25A11, GAPDH*
GO:0051156 - glucose 6-phosphate metabolic process	0.0011172	*GPI, G6PC3, HK2, HK1*
GO:0046835 - carbohydrate phosphorylation	0.00144463	*PFKFB4, POMK, HK2, GNE, HK1*
GO:0033489 - cholesterol biosynthetic process via desmosterol	0.00279114	*EBP, DHCR24, DHCR7*

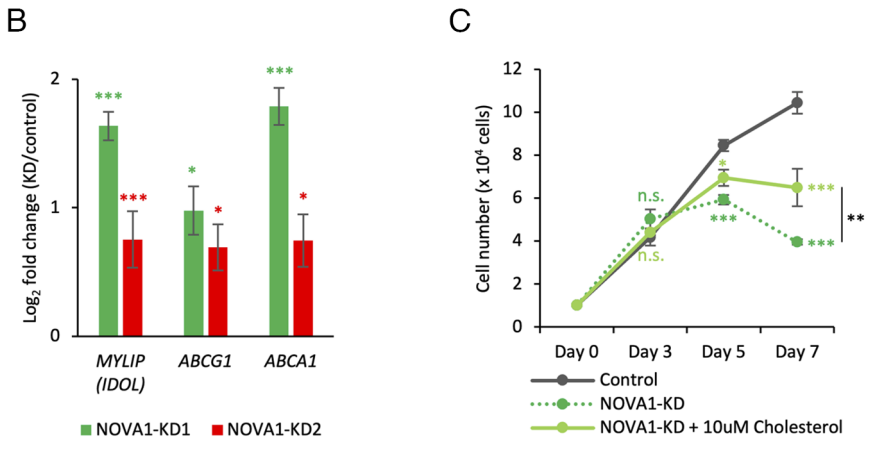

Fig. 4. Dysregulation of cholesterol biosynthetic process genes in NOVA1-KD GBM cell. (*A*) GO terms enriched in the down-regulated genes (FDR < 0.05) in NOVA1-KD GBM cell. (*B*) Quantitative PCR assays for the LXR signaling transcripts in the NOVA1-KD GBM cells (n = 4, **P* < 0.05, ****P* < 0.001). LXR is a transcription factor that promotes cholesterol efflux when activated by cholesterol metabolites or synthetic compounds. (*C*) Comparison of NOVA1-KD GBM cell number treated with or without 10 μM cholesterol. (n = 4, **P* < 0.05, ****P* < 0.001).

binding overlaid Ago2-miRNA CLIP targets. Together, these observations indicate that NOVA1 is able to have strong impacts on 3′UTR miRNA regulation in glioma cells as well as neurons.

Overlapping CLIP binding of NOVA1 and AGO2 could indicate agonistic or antagonistic interactions. The instance observed in mouse brain of NOVA1 overlapping *Impact* 3′UTR elements that were also miRNA binding sites led to the biochemical observation that NOVA1 binding interfered with miRNA binding and correlated with an action of NOVA1 to increase *Impact* mRNA and protein levels. In human GBM cells, the net result of NOVA1 3′UTR binding was to increase target mRNA steady-state levels (Fig. 2*D* and *SI Appendix*, Fig. S2). Importantly, NOVA1 3′UTR binding in human GBM cells was found to be functional at both a mechanistic and biologic level. Generally, the action of NOVA1 binding in 3′UTR to affect steady-state mRNA levels was strongest in transcripts where that binding overlapped AGO2-miRNA binding, suggesting that the general action of NOVA1 binding is likely to antagonize AGO2–miRNA mRNA expression (Fig. 3 *C* and *F*). Although our previous work revealed NOVA1 3′UTR binding participated in the selection of alternative polyadenylation (APA) sites in the mouse brain (22), no clear APA shift of the NOVA1 target transcripts shown in *SI Appendix*, Fig. S2 were found in NOVA1-KD GBM cells. This negative result could result from a variety of causes, ranging from a lack of depth of sequencing to biologic differences in how NOVA regulates APA in neurons and GBM.

At a biologic level, NOVA1 CLIP results reveal a biologically coherent action on transcripts involved in cholesterol metabolism in GBM cells (Fig. 4*A*). Such NOVA1 biologic coherence is reminiscent of observations of coherent actions of NOVA in neurons [on synaptic functions; (19)]. In GBM, prior studies have linked cholesterol metabolism as important components of cancer cell growth, in which cholesterol levels depend on the net results of increased cholesterol uptake and decreased efflux. Paradoxically, GBM cells also down-regulate cholesterol synthesis, likely redirecting metabolism toward other key pathways such as DNA replication and protein production. Accordingly, there is evidence that GBM may rely on these two aspects of cholesterol metabolic pathways, a reduction in cholesterol efflux and an increase in cholesterol uptake (29, 32–34) observations were independently supported through a machine learning approach assessing TCGA data and identifying markedly decreased survival in glioma ($P < 0.013$) in tumors with negative regulation of sterol transport (35). Our findings support the possibility that NOVA1-selective actions on these pathways may impact GBM cell fitness. NOVA1 is able to act in GBM cells to increase cholesterol homeostasis that is essential for GBM cell survival. Taken together, these results suggest the possibility that targeting NOVA1 oncogenic protein–RNA interactions, particularly those involved in the cholesterol biosynthetic pathways, might be clinically relevant, although clearly further studies will be needed as our results were obtained with a patient-derived GBM cell line. One strategy that the precision of our NOVA1 binding sites suggest would be to use ASOs as anti-GBM targets, including interfering with NOVA1-regulated transcripts involved in cholesterol biosynthetic pathways.

Material & Methods

Cell Culture. For all assays, MSK-19 GBM cells were grown in media consisting of Dulbecco's Modified Eagle Medium (DMEM)/F12 (Invitrogen), Neurobasal(−A) (Invitrogen), human-bFGF (20 ng/mL) (Shenandoah Biotech), and human-EGF (20 ng/mL) (Shenandoah). Dishes were coated with 15 μg/mL of Poly-L-ornithine (Millipore: P3655), 2 ug/mL Fibronectin (Corning: CB-40008A), and 4 μg/mL Laminin (R&D Systems: 3400-010-02).

Cell Viability and Proliferation Assay. Proliferation assays were performed in media as above, and cell viability at indicated days were determined using CellTiter-Glo® Luminescent Cell Viability Assay (Promega) or CellTiter-Blue Cell Viability Assay (Promega) according to the manufacturer's guidelines. For cholesterol rescue experiments, water-soluble cholesterol (cholesterol-methyl-β-cyclodextrin, Millipore-Sigma: C4951) was added to cells in culture at the initiation of assay. Then, 0.5 pmol ASOs were treated for 5 d by free uptake.

Xenograft Tumorigenicity Assay. All animal experiments were done in accordance with protocols approved by our Institutional Animal Care and Use Committee and following NIH guidelines for animal welfare. MSK-19 cells were dissociated with Accutase (Innovative Cell Technologies) and the number of live cells was counted by Acridine Orange and Propidium Iodide staining (Nexcelom). MSK-19 cells were resuspended in PBS and 1×10^5 cells were stereotactically transplanted into the brain of NOD/SCID mice (NOD.Cg-Prkdc^{scid} Il2rgtm1Wjl/SzJ; RRID: IMSR_JAX:005557). Male mice were evenly assigned to each group. Coordinates of the injection site were 2 mm lateral and 2 mm posterior to bregma and 2 mm deep from the head skull. Mice were monitored for up to 5 mo. Survival of mice was evaluated by Kaplan–Meier analysis and *P* values were calculated using a log-rank test. For in vivo imaging, cells were lentivirally labeled with luciferase and luminescence was measured using IVIS Spectrum In Vivo Imaging System.

CLIP and Data Analysis. For each independent replicate of NOVA1 and AGO CLIP in MSK-19 GBM cells, 90 to 95% confluent two 10cm dishes were used. Cells were UV-crosslinked in ice-cold PBS with one time 150 mJ/cm2 using a Stralinker (model 2400). CLIP was performed as described previously (25, 36). First, we performed NOVA1 CLIP, and then post NOVA1-CLIP supernatant was used for AGO CLIP. Individual CLIP libraries were multiplexed and sequenced by MiSeq (Illumina) to obtain 75-nt single-end reads. CLIP data analyses were done using the CLIP Tool Kit (37) as described previously. Trimmed CLIP reads were mapped on the hg19 build of the human genome by Burrows–Wheeler Aligner (38). Only unique CLIP tags gotten by collapsing PCR duplicates were used for subsequent analyses. We performed four CLIP replicates. All scripts used in the analysis including the peak finding algorithm and more information can be publicly obtained at (https://zhanglab.c2b2.columbia.edu/index.php/Standard/BrdUCLIP_data_analysis_using_CTK). All identified CITS sites were subjected to NOVA1-binding motif search. De novo motif analysis was done using the MEME-ChIP version 5.4.1 (39) with default parameters for RNA motifs. GO term analysis was done using DAVID (40, 41).

RNAseq and RNAseq Data Analysis. mRNA-seq libraries were prepared from Trizol-extracted RNA following Illumina TruSeq protocols for poly-A selection, fragmentation, and adaptor ligation. Multiplexed libraries were sequenced as 100 nt paired-end runs on Novaseq platforms at the Rockefeller University Genomics Resource Center. Reads were aligned to the hg19 build using STAR (42) and analyzed by differential analysis of raw sequencing counts using DESeq2 (Bioconductor, https://www.bioconductor.org/packages/release/bioc/html/DESeq2.html) (43).

ASOs and Primers. Twenty nucleotide length oligonucleotides (Integrated DNA Technologies) with 2′-*O*-Methyl and phosphorothioate modifications were used. ASO-a: TCAGTGAATGTTAAATGAAG, ASO-b: TAAATGAATGGAATGAGTGA, ASO-c: GTGAAATGATAAATGAATGG, ASO-control: CTAAGGTTAAGTCGCCCTCG. Primer's sequence used for qPCR are ABCA1_F: TCAGGTGCCTTGGCAGTGTC, ABCA1_R: GCTCTGGGAGAGGATGCTGA, ABCG1_F: CCACAGCTTCTCTGCCAGCT, ABCG1_R: CCGCGAACATGAGGAACAGC, MYLIP_F: GCTCTCCTCTGCCACCTTGA, MYLIP_R: AGCAGTTTCTGCCCTTCGCTATC, ACTB_F: ACATTAAGGAGAAGCTGTGCTACG, ACTB_R: GAAGGCTGGAAGAGTGCCTC, GAPDH_F: GTCCATGCCATCACTGCCAC, GAPDH_R: CTCAGGGATGACCTTGCCCA.

Plasmids. For the construction of shRNA-expressing vectors, annealed oligos were cloned into pLKO.1 puro vector digested with AgeI and EcoRI enzymes (Addgene #8453) (44). Target sequences are shNOVA1 #1: ATCAGATGGAGAGGACTTGG, shNOVA1 #2: GATCTGGATTAACGGTGGTCT, shControl: CGAGGGCGACTTAACCTTAGG. For the construction of human NOVA1 expression vector, human NOVA1 CDS was cloned into pCW57.1 (addgene #41393).

qPCR. Extracted RNA with Trizol was reverse transcribed using SuperScript III First-Strand synthesis System for quantitative PCR (Invitrogen; 18080-051). qRT-PCR was performed with FastStart SYBR Green Master (Roche; 04 673 492 001) on BIO-RAD Touch Real-Time PCR Detection System. The following program was

carried to 40 cycles: 30 s 95 °C (denaturation); 30 s 58 °C (annealing); and 20 s 72 °C (extension). Results were analyzed by ΔΔCt, using Actb mRNA for normalization. Semiquantitative RT-PCR was performed as previously described (31).

Lentivirus Production. Lentiviral vectors were transfected in HEK293T cells with packaging vectors (pMD2.G and psPAX2), in the presence of Lipofectamine 3000 (Invitrogen). MD2.G was a gift from Didier Trono (École Polytechnique Fédérale de Lausanne, Lausanne, Switzerland; Addgene plasmid #12259; http://n2t.net/addgene:12259; RRID:Addgene_12259) and psPAX2 was a gift from Didier Trono (École Polytechnique Fédérale de Lausanne, Lausanne, Switzerland; Addgene plasmid #12260; http://n2t.net/addgene:12260; RRID:Addgene_12260). Cultured medium were changed 24 h after transfection and viral supernatants were collected 48 h after medium change and viral particles were concentrated by ultracentrifugation at 49,000 g for 1.5 h at 4 °C.

Antibodies. Primary antibodies used for CLIP were rabbit anti-NOVA1 (1:1,000; Abcam ab183024) and mouse anti-AGO (2A8: gift from Zissimos Mourelatos). Rabbit anti-mouse IgG (Jackson ImmunoResearch 315-005-008) was used as a bridging antibody for Ago CLIP. The following antibodies were used for immunoblots: rabbit anti-NOVA1 (1:1,000; Abcam ab183024), and mouse anti-β-Actin (1:20,000; Abcam ab6276).

Data, Materials, and Software Availability. The RNA sequence data discussed in this publication have been deposited in NCBI's Gene Expression Omnibus (45) and are accessible through GEO Series accession number GSE242124 (https://www.ncbi.nlm.nih.gov/geo/query/acc.cgi?acc=GSE242124).

ACKNOWLEDGMENTS. We thank Darnell lab members for suggestions, expertise, and feedback. This work was supported by funds from NIH awards NS081706 and R35NS097404 (to R.B.D.), and the Starr Cancer Consortium to Y.S., V.T., and R.B.D. (I14-0031). R.B.D. is an Investigator of the Howard Hughes Medical Institute.

Author affiliations: [a]HHMI, The Rockefeller University, New York, NY 10065; [b]Laboratory of Molecular Neuro-oncology, The Rockefeller University, New York, NY 10065; [c]Department of Neurosurgery, Center for Stem Cell Biology, Memorial Sloan Kettering Cancer Center, New York, NY 10065; and [d]Cancer Biology and Genetics, Sloan Kettering Institute, New York, NY 10065

1. R. J. Buckanovich, J. B. Posner, R. B. Darnell, Nova, the paraneoplastic Ri antigen, is homologous to an RNA-binding protein and is specifically expressed in the developing motor system. *Neuron* **11**, 657–672 (1993).
2. R. B. Darnell, J. B. Posner, Paraneoplastic syndromes involving the nervous system. *N. Engl. J. Med.* **349**, 1543–1554 (2003).
3. R. B. Darnell, F. J B. Posner MD, *Paraneoplastic Syndromes* (Oxford University Press, 2011).
4. R. B. Darnell, J. B. Posner, Observing the invisible: Successful tumor immunity in humans. *Nat. Immunol.* **4**, 201 (2003).
5. R. B. Darnell, Onconeural antigens and the paraneoplastic neurologic disorders: At the intersection of cancer, immunity, and the brain. *Proc. Natl. Acad. Sci. U.S.A.* **93**, 4529–4536 (1996).
6. Y. Y. Yang, G. L. Yin, R. B. Darnell, The neuronal RNA-binding protein Nova-2 is implicated as the autoantigen targeted in POMA patients with dementia. *Proc. Natl. Acad. Sci. U.S.A.* **95**, 13254–13259 (1998).
7. D. L. Eizirik *et al.*, The human pancreatic islet transcriptome: Expression of candidate genes for type 1 diabetes and the impact of pro-inflammatory cytokines. *PLoS Genet.* **8**, e1002552 (2012).
8. O. Villate *et al.*, Nova1 is a master regulator of alternative splicing in pancreatic beta cells. *Nucleic Acids Res.* **42**, 11818–11830 (2014).
9. R. B. Darnell, L. M. DeAngelis, Regression of small-cell lung carcinoma in patients with paraneoplastic neuronal antibodies. *Lancet* **341**, 21–22 (1993).
10. M. L. Albert, R. B. Darnell, Paraneoplastic neurological degenerations: Keys to tumour immunity. *Nat. Rev. Cancer* **4**, 36–44 (2004).
11. W. K. Roberts, R. B. Darnell, Neuroimmunology of the paraneoplastic neurological degenerations. *Curr. Opin. Immunol.* **16**, 616–622 (2004).
12. F. A. Luque *et al.*, Anti-Ri: An antibody associated with paraneoplastic opsoclonus and breast cancer. *Ann. Neurol.* **29**, 241–251 (1991).
13. M. L. Suvà *et al.*, Reconstructing and reprogramming the tumor-propagating potential of glioblastoma stem-like cells. *Cell* **157**, 580–594 (2014).
14. R. B. Darnell, RNA protein interaction in neurons. *Annu. Rev. Neurosci.* **36**, 243–270 (2013).
15. B. K. Dredge, G. Stefani, C. C. Engelhard, R. B. Darnell, Nova autoregulation reveals dual functions in neuronal splicing. *EMBO J.* **24**, 1608–1620 (2005).
16. K. B. Jensen *et al.*, Nova-1 regulates neuron-specific alternative splicing and is essential for neuronal viability. *Neuron* **25**, 359–371 (2000).
17. R. J. Buckanovich, Y. Y. Yang, R. B. Darnell, The onconeural antigen Nova-1 is a neuron-specific RNA-binding protein, the activity of which is inhibited by paraneoplastic antibodies. *J. Neurosci.* **16**, 1114–1122 (1996).
18. M. Ruggiu *et al.*, Rescuing Z+ agrin splicing in Nova null mice restores synapse formation and unmasks a physiologic defect in motor neuron firing. *Proc. Natl. Acad. Sci. U.S.A.* **106**, 3513–3518 (2009).
19. J. Ule *et al.*, Nova regulates brain-specific splicing to shape the synapse. *Nat. Genet.* **37**, 844–852 (2005).
20. Y. Tajima *et al.*, NOVA1 acts on Impact to regulate hypothalamic function and translation in inhibitory neurons. *Cell Rep.* **42**, 112050 (2023).
21. J. Ule *et al.*, CLIP identifies Nova-regulated RNA networks in the brain. *Science* **302**, 1212–1215 (2003).
22. D. D. Licatalosi *et al.*, HITS-CLIP yields genome-wide insights into brain alternative RNA processing. *Nature* **456**, 464–469 (2008).
23. J. Ule, H.-W. Hwang, R. B. Darnell, The future of cross-linking and immunoprecipitation (CLIP). *Cold Spring Harb. Perspect. Biol.* **10**, a032243 (2018).
24. C. Zhang, R. B. Darnell, Mapping in vivo protein-RNA interactions at single-nucleotide resolution from HITS-CLIP data. *Nat. Biotechnol.* **29**, 607–614 (2011).
25. Y. Saito *et al.*, NOVA2-mediated RNA regulation is required for axonal pathfinding during development. *Elife* **5**, e14371 (2016).
26. T. Eom *et al.*, NOVA-dependent regulation of cryptic NMD exons controls synaptic protein levels after seizure. *Elife* **2**, e00178 (2013).
27. C. Zhang *et al.*, Integrative modeling defines the Nova splicing-regulatory network and its combinatorial controls. *Science* **329**, 439–443 (2010).
28. S. W. Chi, J. B. Zang, A. Mele, R. B. Darnell, Argonaute HITS-CLIP decodes microRNA-mRNA interaction maps. *Nature* **460**, 479–486 (2009).
29. D. Guo *et al.*, An LXR agonist promotes glioblastoma cell death through inhibition of an EGFR/AKT/SREBP-1/LDLR-dependent pathway. *Cancer Discov.* **1**, 442–456 (2011).
30. I. M. Capell-Hattam, N. M. Fenton, H. W. Coates, L. J. Sharpe, A. J. Brown, The non catalytic protein ERG28 has A functional role in cholesterol synthesis and is coregulated transcriptionally. *J. Lipid Res.* **63**, 100295 (2022).
31. R. E. Phillips *et al.*, Target identification reveals lanosterol synthase as a vulnerability in glioma. *Proc. Natl. Acad. Sci. U.S.A.* **116**, 7957–7962 (2019).
32. D. Patel *et al.*, LXRβ controls glioblastoma cell growth, lipid balance, and immune modulation independently of ABCA1. *Sci. Rep.* **9**, 15458 (2019).
33. D. Li, S. Li, A. Z. Xue, L. A. Smith Callahan, Y. Liu, Expression of SREBP2 and cholesterol metabolism related genes in TCGA glioma cohorts. *Medicine* **99**, e18815 (2020).
34. F. Ahmad, Q. Sun, D. Patel, J. M. Stommel, Cholesterol metabolism: A potential therapeutic target in glioblastoma. *Cancers* **11**, 146 (2019).
35. M. Garbulowski *et al.*, Machine learning-based analysis of glioma grades reveals co-enrichment. *Cancers* **14**, 1014 (2022).
36. Y. Saito *et al.*, YTHDC2 control of gametogenesis requires helicase activity but not m6A binding. *Genes. Dev.* **36**, 180–194 (2022).
37. A. Shah, Y. Qian, S. M. Weyn-Vanhentenryck, C. Zhang, CLIP Tool Kit (CTK): A flexible and robust pipeline to analyze CLIP sequencing data. *Bioinformatics* **33**, 566–567 (2017).
38. H. Li, R. Durbin, Fast and accurate short read alignment with Burrows-Wheeler transform. *Bioinformatics* **25**, 1754–1760 (2009).
39. P. Machanick, T. L. Bailey, MEME-ChIP: Motif analysis of large DNA datasets. *Bioinformatics* **27**, 1696–1697 (2011).
40. D. W. Huang, B. T. Sherman, R. A. Lempicki, Systematic and integrative analysis of large gene lists using DAVID bioinformatics resources. *Nat. Protoc.* **4**, 44–57 (2009).
41. B. T. Sherman *et al.*, DAVID: A web server for functional enrichment analysis and functional annotation of gene lists (2021 update). *Nucleic Acids Res.* **50**, W216–W221 (2022).
42. A. Dobin *et al.*, STAR: Ultrafast universal RNA-seq aligner. *Bioinformatics* **29**, 15–21 (2013).
43. M. I. Love, W. Huber, S. Anders, Moderated estimation of fold change and dispersion for RNA-seq data with DESeq2. *Genome Biol.* **15**, 550 (2014).
44. S. A. Stewart *et al.*, Lentivirus-delivered stable gene silencing by RNAi in primary cells. *RNA* **9**, 493–501 (2003).
45. R. Edgar, M. Domrachev, A. E. Lash, Gene Expression Omnibus: NCBI gene expression and hybridization array data repository. *Nucleic Acids Res.* **30**, 207–210 (2002).